SCIENCE AND TECHNOLOGY OF ADVANCED MATERIALS, 2016
VOL. 17, NO. 1, 736–743
http://dx.doi.org/10.1080/14686996.2016.1244474

Taylor & Francis
Taylor & Francis Group

OPEN ACCESS

A study of the optical and polarisation properties of InGaN/GaN multiple quantum wells grown on *a*-plane and *m*-plane GaN substrates

Dmytro Kundys[a], Danny Sutherland[a], Matthew J. Davies[a], Fabrice Oehler[b], James Griffiths[b], Philip Dawson[a], Menno J. Kappers[b], Colin J. Humphreys[b], Stefan Schulz[c], Fengzai Tang[b] and Rachel A. Oliver[b]

[a]School of Physics and Astronomy, Photon Science Institute, University of Manchester, Manchester, UK
[b]Department of Materials Science and Metallurgy, University of Cambridge, Cambridge, UK
[c]Photonics Theory Group, Tyndall National Institute, Cork, Ireland

ABSTRACT

We report on a comparative study of the low temperature emission and polarisation properties of InGaN/GaN quantum wells grown on nonpolar $(11\bar{2}0)$ *a*-plane and $(10\bar{1}0)$ *m*-plane free-standing bulk GaN substrates where the In content varied from 0.14 to 0.28 in the *m*-plane series and 0.08 to 0.21 for the *a*-plane series. The low temperature photoluminescence spectra from both sets of samples are broad with full width at half maximum height increasing from 81 to 330 meV as the In fraction increases. Photoluminescence excitation spectroscopy indicates that the recombination mainly involves strongly localised carriers. At 10 K the degree of linear polarisation of the *a*-plane samples is much smaller than of the *m*-plane counterparts and also varies across the spectrum. From polarisation-resolved photoluminescence excitation spectroscopy we measured the energy splitting between the lowest valence sub-bands to lie in the range of 23–54 meV for the *a*- and *m*-plane samples in which we could observe distinct exciton features. Thus the thermal occupation of a higher valence sub-band cannot be responsible for the reduction of the degree of linear polarisation at 10 K. Time-resolved spectroscopy indicates that in *a*-plane samples there is an extra emission component which is at least partly responsible for the reduction in the degree of linear polarisation.

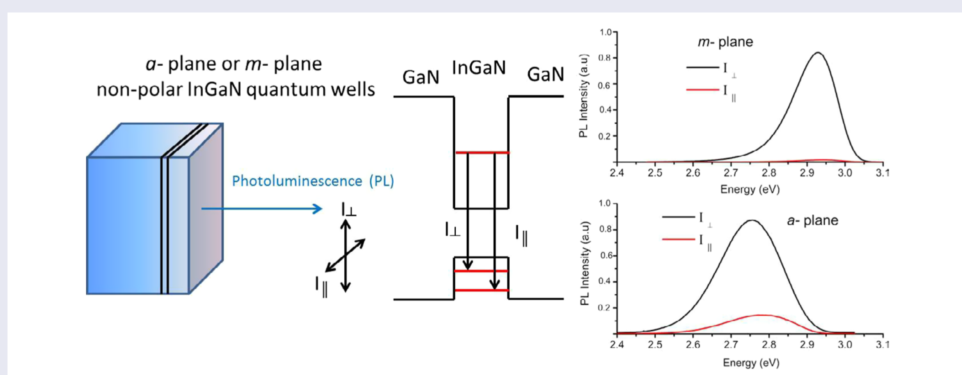

ARTICLE HISTORY
Received 12 May 2016
Revised 23 September 2016
Accepted 27 September 2016

KEYWORDS
InGaN; quantum wells; polarised light; non-polar

CLASSIFICATION
40 Optical, magnetic and electronic device materials; 201 Electronics/Semiconductor/TCOs; 204 Optics/Optical applications; 105 Low-Dimension (1D/2D) materials

1. Introduction

Nonpolar InGaN/GaN multiple quantum wells (MQWs) are attracting a great deal of interest because of their ability to emit linearly polarised light. This characteristic may be of practical use in e.g. back-lit liquid crystal displays.[1] The emission of polarised light occurs because of the breaking of the crystal symmetry due to anisotropic in-plane strain and differences in the effective hole masses along the growth direction.[2,3] The degree of optical linear polarisation (DLP) of the total light emission ideally should depend on the relative populations of the two lowest energy valence sub-bands. The DLP of the emission is defined (in terms of the geometry of our experiment; see Figure 1) as follows:

$$\mathrm{DLP} = \frac{(I_{\perp} - I_{\parallel})}{(I_{\perp} + I_{\parallel})} \quad (1)$$

For any application that relies on polarised light it is not only vital that the DLP be high but also the efficiency of the intrinsic emission be as large as possible. This latter issue can be affected by the choice of substrate. Various substrates are available for heteroepitaxial growth of nonpolar GaN such as SiC,[4] $LiAlO_3$ [5] and

CONTACT Philip Dawson Philip.dawson@manchester.ac.uk

© 2016 The Author(s). Published by National Institute for Materials Science in partnership with Taylor & Francis.
This is an Open Access article distributed under the terms of the Creative Commons Attribution License (http://creativecommons.org/licenses/by/4.0/), which permits unrestricted use, distribution, and reproduction in any medium, provided the original work is properly cited.

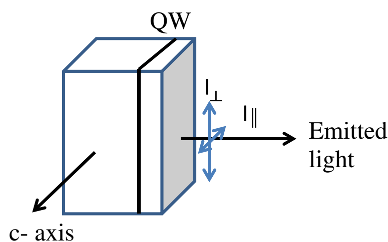

Figure 1. Diagram showing the definition of the polarisations of light ($I_\perp$) perpendicular and ($I_\parallel$) parallel to the *c*-axis.

sapphire.[6–9] Heteroepitaxial growth, however, results in high densities of extended defects, despite the use of sophisticated defect reduction techniques.[10,11] Typically the densities of threading dislocations and basal plane stacking faults for heteroepitaxial non-polar growth are (2–7) × 10^9 cm^{-2} and ~10^5 cm^{-1}respectively.[12] Such high densities of defects can lead to extrinsic non-radiative and radiative processes that reduce the efficiency of the intrinsic emission process. For these reasons the most promising choice for high efficiency, large DLP structures is homoepitaxial growth on freestanding, ammonothermal GaN substrates with a threading dislocation density lower than 10^5 cm^{-2} and negligible basal plane stacking faults.

At the moment InGaN/GaN QWs grown on *m*-plane GaN repeatedly show superior polarisation properties with DLP values over 90% at room temperature [13] compared with structures grown on *a*-plane GaN.[14,15] From a theoretical point of view [16] the change of nonpolar plane should make no difference to the polarisation properties of InGaN/GaN QWs. At the moment this behaviour is not understood. In this paper we report on a study of the optical and polarisation properties InGaN/GaN QWs grown on ammonothermal *a*- and *m*-plane GaN substrates. We have used a combination of polarised photoluminescence (PL) spectroscopy, time resolved spectroscopy and polarisation resolved photoluminescence excitation (P-PLE) spectroscopy to compare the properties of the QWs where the differences between the sample sets are entirely due to the growth on the different non-polar planes.

2. Experimental details

All the samples were grown by metalorganic vapour phase epitaxy in a 6 × 2″ Thomas Swan close-coupled showerhead reactor. The five period InGaN/GaN MQW samples were grown on nonpolar ammonothermal GaN substrates with intentional crystal misorientations for the $(11\bar{2}0)$ *a*-plane of 0 ± 0.2° along the *m*-axis and 0.3 ± 0.2° towards the + *c*-axis, and for $(10\bar{1}0)$ *m*-plane 0 ± 0.2° along the *a*-axis and 2.0 ± 0.2° towards the (-*c*)-axis. Trimethylgallium (TMG), trimethylindium (TMI) and ammonia (NH_3) were used as the precursors with hydrogen as the carrier gas for the growth of the GaN epilayer and nitrogen for the growth of InGaN QWs and GaN barrier layers. First, a GaN buffer layer with a thickness of 800 to 1000 nm was grown at 1050 °C followed by the InGaN/GaN QW stacks which were grown using a 'quasi-two temperature' growth method, adapted from a method commonly used for growth on *c*-plane.[17] For the majority of the samples studied the In composition of the samples was varied by changes in the growth temperature from 690 °C to 705 °C for the *a*-plane samples and 705 °C to 745 °C for the *m*-plane samples (see Table 1). It should be noted that A3 and A4 were cut from regions of the same sample that was grown at a nominal growth temperature of 690 °C with A3 coming from a region of the sample where the growth temperature was somewhat higher than the region from which A4 originated.

Following the growth of the InGaN QWs a 1.0 nm GaN cap was grown at the InGaN growth temperature. The TMG and NH_3 flows were then maintained during a 90 s temperature ramp to 860 °C, at which point the barrier growth was completed. Every sample was analysed using a high resolution X-ray diffraction (XRD) MRD diffractometer from Panalytical (Cambridge, United Kingdom), equipped with a symmetric four-bounce monochromator and a three-bounce analyser to select the CuKα1 wavelength. The well and barrier widths and QW compositions (as detailed in Table 1) were determined using ω-2θ scans of the brightest symmetric reflection with a range of 10° in ω following the approach of Vickers et al. [18] and modified for nonpolar orientations.[19] The missing satellite peaks typically present

Table 1. *m*-plane (M series) and *a*-plane (A series) growth temperature and sample properties obtained from XRD and TEM along with optical data measured at 10K.

Sample number	Nominal growth temperature of InGaN (°C)	In fraction	Thickness of QWs (nm)	GaN barrier thickness (nm)	Peak emission energy (eV)	FWHM (meV)	Stokes shift (meV)	Exciton splitting (meV)
M1	745	0.14	1.9	6.1	3.038	121	134±2	38 ± 2
M2	735	0.18	2.0	6.1	2.928	133	180±3	35 ± 4
M3	725	0.22	2.1	6.1	2.802	160	264±4	54 ± 5
M4	705	0.28	2.4	6.1	2.610	157	–	–
A1	705	0.08	2.0	6.0	3.194	81	87±2	23 ± 2
A2	695	0.13	2.1	6.0	2.980	136	137±2	38 ± 2
A3	690	0.16	2.25	6.0	2.765	208	276±4	48 ± 5
A4	690	0.21	2.4	6.0	2.527	330	–	–

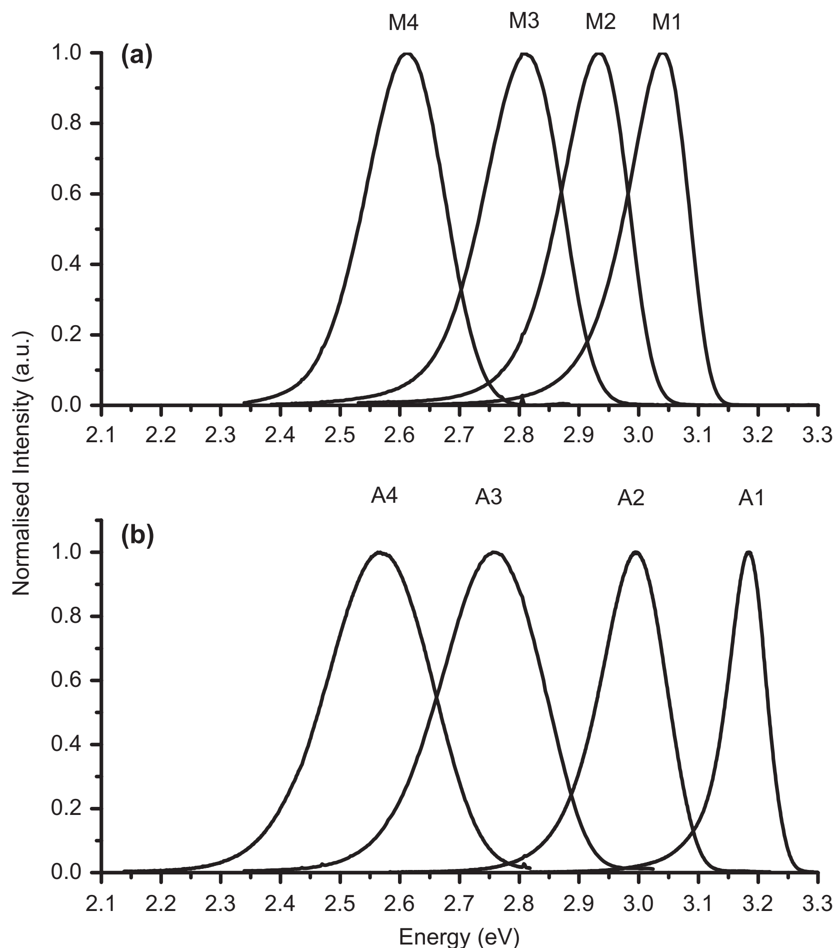

Figure 2. Photoluminescence spectra measured at 10 K are shown in (a) and (b) for *m*-plane and *a*-plane samples respectively identified by the numbers in Table 1.

in XRD scans of MQW structures used to determine the well widths were absent for these samples. Hence, high angle annular dark field scanning transmission electron microscopy (HAADF-STEM) was used to measure the well and barrier widths of samples A2, A4, and M2 to inform the calculation of the layer thicknesses in the remaining samples. HAADF-STEM was performed with an FEI Titan fitted with both probe and image aberration correctors operated at 300 keV. The results of the structural analysis are shown in Table 1.

The PL and P-PLE studies were carried out either using excitation from a CW He/Cd laser or a combination of a 300 W xenon lamp and monochromator as a fixed or tuneable wavelength excitation source respectively. The samples were mounted in the cryostat so that *c*-axis of the GaN was horizontal. The PL from the samples was analysed by a 0.85 m double grating spectrometer and a Peltier-cooled GaAs photomultiplier using standard lock-in detection techniques. The spectral dependence of the degree of polarisation (DLP(E)) of the emission was determined by measuring the PL spectra polarised parallel ($I_{\parallel}$) and perpendicular ($I_{\perp}$) to the *c*-axis of the sample in question and then combining the polarised spectra as described by Equation (1).

The polarisation dependent excitation spectroscopy reveals exciton transitions associated with the different valence sub-bands; this not only enables measurement of the valence sub-band energy splitting as described previously [3,20–23] but can also be used to help to identify the nature of the recombination processes. For the time-resolved PL and PL decay time measurements, a frequency doubled mode-locked Ti:sapphire laser operating at a repetition rate of 800 kHz and emitting light with a photon energy of 3.18 eV was used as the excitation source and the signal processed with a time-correlated single photon counting system.

3. Results and discussion

Figure 2(a) and 2(b) show low temperature (T = 10 K) PL spectra for the InGaN/GaN MQW samples grown on *m*- and *a*-planes respectively. The most noticeable aspect of all the PL spectra is the particularly large line widths which, depending on the In fraction, lie in the range 81 to 330 meV (see Table 1). These line widths are much larger than the equivalent InGaN/GaN QWs grown on *c*-plane substrates, e.g. a polar InGaN/GaN single QW structure with an In fraction of 0.25 exhibited [24] a low

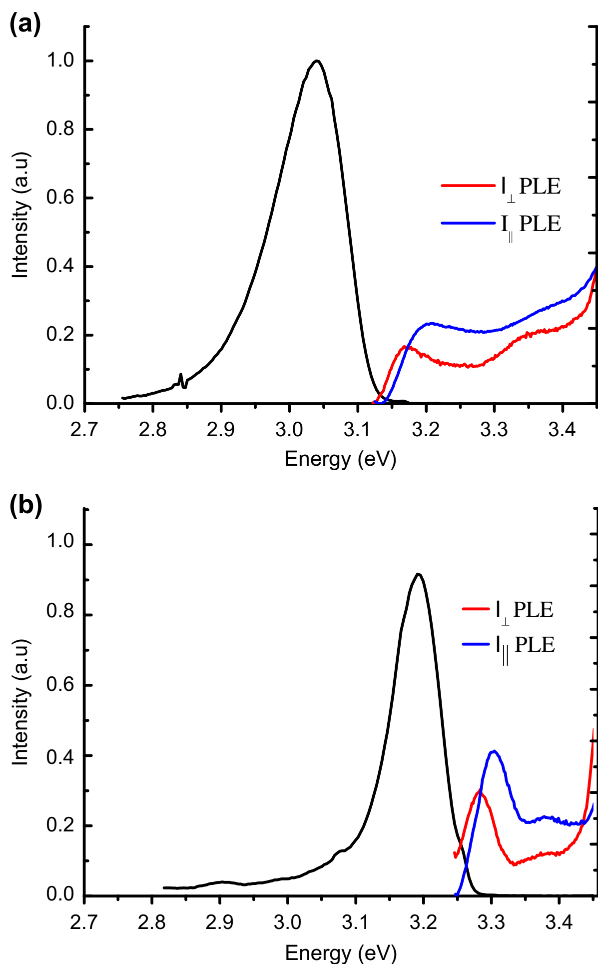

Figure 3. Low temperature (10 K) PL spectra (black line) with PLE spectra are shown in (a) and (b) for *m*- and *a*-plane samples M1 and A1 respectively, for two different linear polarisations of excitation radiation.

temperature PL linewidth of 82 meV whereas A4 and M3 (samples with similar In fractions) have linewidths of 330 and 160 meV respectively. One cause of the large linewidths could be inter-well variations in the In fraction and/or QW thickness. However for the *a*- plane samples this is certainly not the case as the linewidth of a single QW structure grown under the same conditions as a MQW structure had similar spectroscopic characteristics.

A comparison of the P-PLE spectra and the PL spectra throws light on the nature of the dominant recombination process. We were only able to observe distinct exciton transitions associated with the two lowest valence sub-bands in samples M1, M2, M3, A1, A2 and A3. For the samples A4 and M4 the P-PLE spectra were inhomogeneously broadened to such an extent that discrete exciton peaks could not be resolved. The P-PLE spectra for samples M1 and A1 are shown in Figure 3. We attribute the peaks that lie between 3.05 eV and 3.35 eV to exciton transitions involving the $n = 1$ confined electron states and the $n = 1$ confined strain and crystal field split valence bands. Assuming growth along the x-axis and since the crystal field splitting energy in InN and GaN is positive and shifts the |Z>-like valence band states to lower energies compared to the valence band maximum, one expects that the first valence sub-band at k = 0 is mainly |Y>-like in character while the second sub-band being mainly of |Z>-like character. This sub-band level structure is consistent with the measured P-PLE spectrum shown in Figure 3. Furthermore, the magnitude of the splitting between the peaks is consistent with the values reported [25,26] for the crystal field splitting in InN (19–24 meV) and GaN (9–38 meV). The most striking aspect of the data shown in Table 1 are the very large values, as illustrated in particular in Figure 3, for the Stokes shifts between the energies of the lowest energy QW exciton transition and the peak energy of the PL emission. Previously the emission at low temperatures from non-polar InGaN/GaN QWs has been attributed to localised exciton recombination.[27] On this basis the values of the Stokes shifts suggest very large exciton localisation energies that increase with increasing In fraction. It is also noticeable that the linewidths of the exciton features in the P-PLE spectrum are much smaller than the PL line width, e.g. in the case of the data presented in Figure 3(a) the linewidth of the lowest energy exciton peak is ~60 meV in the P-PLE spectrum compared with a PL linewidth of 128 meV. One possible interpretation for this observation is as follows: the exciton transitions in the P-PLE spectrum are associated with the creation of excitons that are free in the plane of the QWs.

If the length scale of the localised disorder is less than the in-plane exciton Bohr radius so that, to an extent, in the PLE spectra the effects of the disorder are averaged out. Yet when the carriers become localised the localisation itself introduces an energy variation at the different localisation sites, perhaps due to variations in quantum confinement in the plane of the QWs.

The nature of the localisation is currently under investigation, but as in polar *c*-plane InGaN/GaN QWs,[28,29] it is probable that the effects of the local concentration of In atoms play a dominant role. In the *c*-plane case these local variations in indium content are mainly statistical fluctuations in a random alloy and indeed recent theoretical modelling [30] has indicated that in *m*-plane QWs hole localisation at random In fluctuations is largely responsible for the low temperature PL linewidth. The major difference between polar and non-polar QWs of course is the absence of an electric field perpendicular to the plane of the QWs, an effect that strongly influences the radiative recombination dynamics in polar structures.[31] However, as demonstrated recently [30] the absence of the electric field has significant consequences for the electron localisation. In polar structures the electric field results in the electrons being localised largely by the well width fluctuations, while in non-polar structures this effect is greatly reduced so that the electrons become bound to the localised holes resulting in localised excitons.

Also of importance is the fact that the P-PLE data reveal directly (assuming no difference in exciton

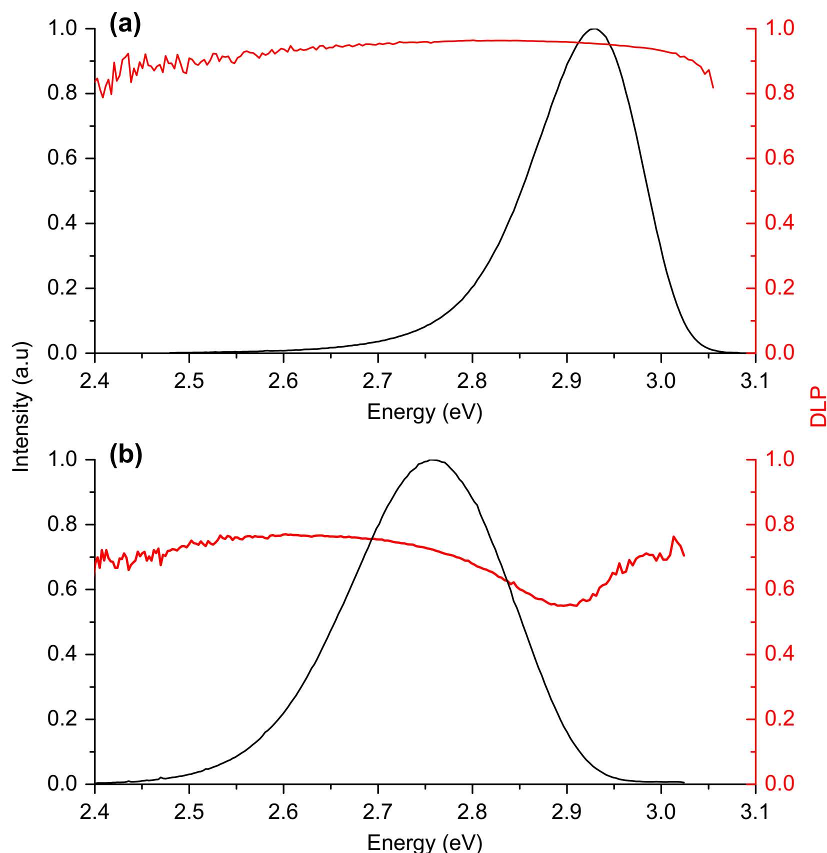

Figure 4. Photoluminescence spectra (black solid lines) and corresponding spectral dependence of the DLP (red line) measured at 10 K are shown in (a) and (b) for *m*-plane and *a*-plane samples M3 and A3 respectively.

binding energies for the different valence bands) the energy difference of the two lowest lying valence bands. For the samples in which we were able to determine the exciton splitting (listed in Table 1) the values are 23 ± 2 meV (A1), 35 ± 5 meV (A2), 48 ± 5 meV (A3), 38 ± 2 meV (M1), 35 ± 4 meV (M2) and 54 ± 5 meV (M3). Following the discussion above about the expected valence sub-band structure in non-polar InGaN QWs, the magnitude of the measured splitting is, to a first approximation, consistent with the magnitudes one could expect from InGaN crystal field splitting energies. Obviously strain effects and differences in effective masses along the growth direction can also affect the relative energetic positions of the different valence sub-bands. However, the measured values strengthen the argument that the P-PLE data gives direct insight into the energy difference of the first two valence sub-bands. Furthermore, these values are similar to those reported elsewhere [13,21,22,32] from polarised PL and electroluminescence measurements on InGaN QW structures. Although it should be born in mind that a direct comparison of the values reported here and those in the cited works is not strictly valid. This is because the data reported here essentially reflect the differences between the free exciton transitions associated with the different valence sub-bands whereas the referenced data consist of measurements involving recombination that could well be influenced by the effects of carrier localisation.

Figure 4 shows the spectral dependences of the DLP(E) for the *a*- and *m*-plane samples A3 and M2; it should be stressed that contrasting spectra are representative of the behaviour from the two sample sets. The *m*-plane sample exhibits a high value of DLP (>0.9) which is constant across the spectrum, but the *a*-plane sample exhibits a maximum value of the DLP ~0.6 and the DLP(E) spectrum with a pronounced reduction on the high energy side of the spectrum. The first question to ask is whether there is any evidence for a difference in the lowest energy valence sub-band splitting in the *m*- and *a*-plane structures which could influence the DLP in the different structures. As described above the values of the valence sub-band splitting in the *a*- and *m*-plane samples in which we were able to observe any exciton transitions are ≥23 meV. So ignoring any effects due to localisation we conclude at a temperature of 10 K that the higher lying valence states are not significantly occupied for both *a*- and *m*-plane samples. Hence the differences in the DLP and the spectral dependence cannot be explained by differences in the splitting of the valence sub-band energies. As implied above this argument ignores the nature of the recombination and really would only valid for the case of free carrier recombination. As we have already noted this is not the case at a temperature of 10 K with the recombination of localised excitons likely to be dominant. As to the dip in the DLP(E) for the *a*-plane samples, if we examine the PL

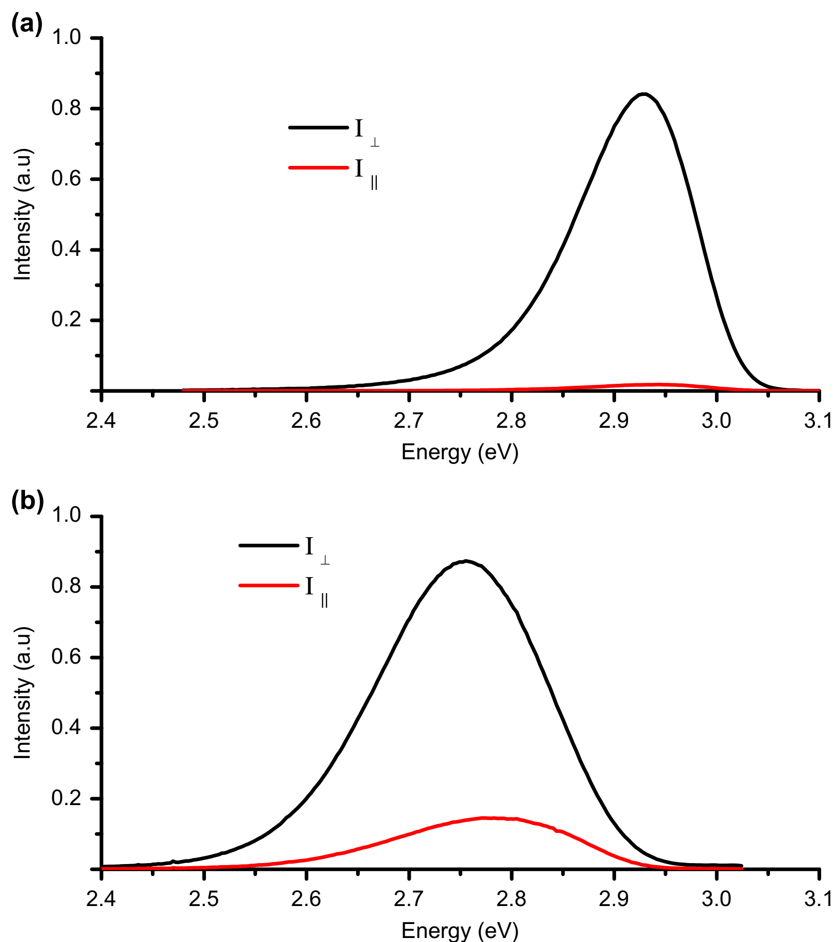

Figure 5. PL spectra for (a) M2 and (b) A3 detected when monitoring light with polarisations in the $I_{\perp}$ and $I_{\parallel}$ directions as indicated.

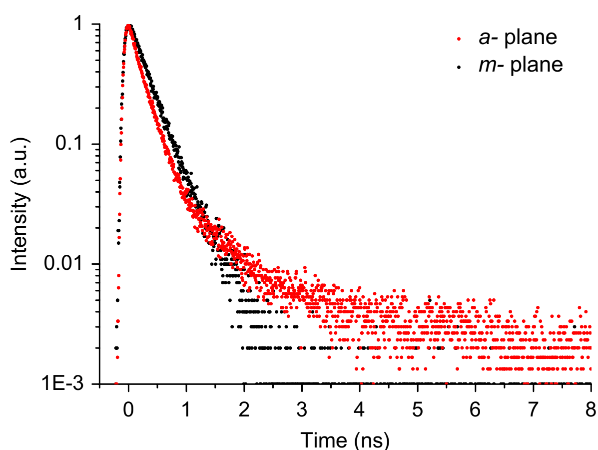

Figure 6. PL time decay curves for samples M2 and A3 as indicated in the figure.

spectra for the two polarisations as shown in Figure 5 there is a clear difference in the peak position of the two spectra. This in itself does not necessarily suggest that there are two distinct recombination channels for the *a*-plane samples; in fact it merely represents how the DLP changes across the spectrum. We can also plot the DLP data in the form shown in Figure 5 where the spectra for both polarisations are plotted separately for an *a*-plane and an *m*-plane structure. These plots reveal that the mechanism responsible for both the low DLP and the dip in the DLP(E) spectrum of the *a*-plane sample is common to both the *a*- and *m*-plane structures, with whatever the cause of this behaviour being much less important in the *m*-plane samples.

To throw further light on the differences in the spectral dependence of the polarisation data of the *a*- and *m*-plane samples we performed PL time decay measurements and time-resolved spectroscopy. The time decay data measured at the peak of the spectra for samples M2 and A3 are shown in Figure 6. All the *m*-plane samples exhibit single exponential decays with time constants ~300 ps which remain unchanged across the individual spectra. This is similar to the data that have already been reported elsewhere.[25]

However, the PL decay curves from the *a*-plane samples exhibit an additional component that decays over a much longer time scale. It should also be noted that the time constant of the rapidly decaying component from the *a*-plane sample is very similar to that measured on the *m*-plane sample, implying that the majority of the emission from the *a*- and *m*-plane samples involves an identical recombination process. Also the longer lived component increases in relative strength as the detection energy is moved to the high energy side of the spectrum. The results of the time resolved spectroscopy shown in Figure 7 reflect this observation. In the time window 0–1 ns where the decay is dominated

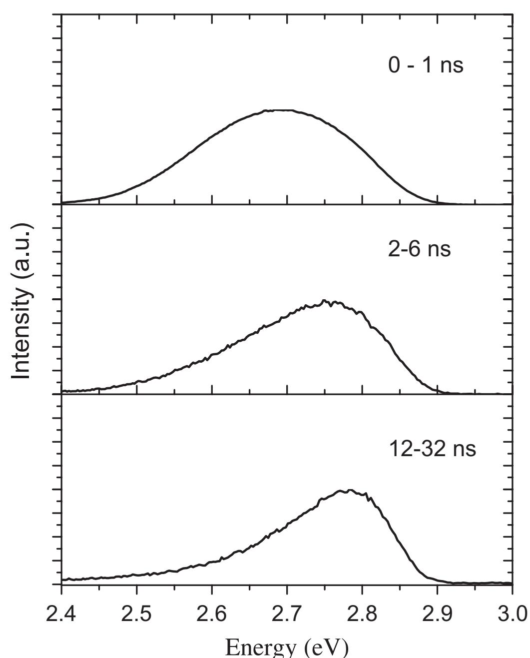

Figure 7. Time resolved spectra for sample A3 for the time windows indicated after the laser pulse which occurred at $t = 0$.

by the fast component the emission spectrum is very similar to the CW spectrum in Figure 2(b). Whereas as the time window is moved to longer times after the laser pulse there is a clear shift of the peak of the spectrum to higher energy.

The nature of the long lived emission component and its role in reducing the DLP is far from clear at the moment and we can only speculate about the processes responsible. Clearly in both the *a*- and *m*-plane samples carrier localisation plays a big role in not only determining the form of the PL spectra but also the recombination energy. This leads us to suggest that in the *a*-plane samples the localisation itself in some parts of the QWs may not only perturb the nature of the localised hole states but may also influence the electron/hole pair configuration reducing the radiative recombination rate. We are currently examining the nanoscale structure of the QWs grown on *a*- and *m*-plane surfaces in some detail to try to elucidate structural differences which may help to explain the different optical properties observed for the two non-polar orientations.

Structural aspects under investigation include the possibility of non-random indium clustering within the QWs. As we discuss elsewhere,[30,33] samples A2 and M1 have been examined using atom probe tomography (APT), revealing differences in the homogeneity of the indium distribution, with a stronger tendency to clustering in the *a*-plane sample. This is consistent with our earlier APT observations of clustering for *a*-plane InGaN QWs grown on ELOG substrates.[34] Furthermore, other groups have reported that *m*-plane QWs are homogeneous.[35] Another aspect of interest is the structure of the InGaN/GaN interfaces in terms of both surface step-related kinetic roughening process and potentially of the formation of three-dimensional quantum dots. Although the dataset we are developing is complex and the differences between *a*- and *m*-plane samples are not yet fully understood, initial indications are that for the same indium content, *a*-plane samples are more likely to both exhibit non-random indium clustering and have rougher surfaces than *m*-plane samples. This is contrary to the situation in *m*-structures in which no evidence of In clustering has been reported.[34] Both these factors, and possibly other microstructural issues, could potentially contribute to the explanation of the differences in optical properties between the two families of samples, particularly since it is the *a*-plane materials which deviate most markedly from the expected optical behaviour and also exhibits the greatest microstructural disorder compared to a theoretical QW of uniform composition and width. Our recent atomistic [30] theoretical work on *m*-plane InGaN/GaN QWs indicated that the microstructure can play an important role in the mixing of different orbital contributions and resulting therefore in a reduced DLP. In the theoretical work on *m*-plane structures a random alloy assumption was made, clustering effects might further enhance these orbital mixing effects and explain therefore the observed reduced DLP in the *a*-plane samples. A more detailed microstructural analysis will be the subject of a later publication.

4. Summary

In summary we observed that the maximum DLP of the *a*-plane QW samples is much less than that observed in the *m*-plane samples. Detailed studies of the spectral dependence of the DLP along with time decay measurements and time resolved spectroscopy revealed that the lower DLP of the *a*-plane samples compared with the *m*-plane samples is associated with an additional underlying emission band. As our comparison of the exciton transitions in the PLE spectra with the peak energies of the recombination reveal the effects of very strong localisation we speculate that the underlying emission band in the *a*-plane samples is due to some change in the localisation environment. The data associated with the paper are openly available from The University of Manchester eScholar Data Repository: http://dx.doi.org/10.15127/1.304121.

Disclosure statement

No potential conflict of interest was reported by the authors.

Funding

This work was supported by UK Engineering and Physical Sciences Research Council [grant numbers EP\J001627\1, EP\J003603\1]; and Science Foundation Ireland [grant number 13/SIRG/2210].

References

[1] Matsui H, Fellows NN, Nakamura S, et al. Optical polarization characteristics of light emission from sidewalls of primary-color light-emitting diodes. Semicond Sci Technol. 2008;23:072001–072005.

[2] Waltereit P, Brandt O, Trampert A, et al. Nitride semiconductors free of electrostatic fields for efficient white light-emitting diodes. Nature. 2000;406:865–868.

[3] Schulz S, Badcock TJ, Moram MA, et al. Electronic and optical properties of non-polar a-plane GaN quantum wells. Phys Rev B, 2010;82:125318-1–125318-13

[4] Sun Q, Yerino CD, Zhang Y, et al. Effect of NH3 flow rate on m-plane GaN growth on m-plane SiC by metalorganic chemical vapor deposition. J Cryst Growth. 2009;311:3824–3829.

[5] Iwata K, Asahi H, Asami K, et al. Gas source molecular beam epitaxy growth of gan on C-, A-, R- and M-plane sapphire and silica glass substrates. Jpn J Appl Phys. 1997;36:L661–L664.

[6] Johnston CF, Kappers MJ, Barnard JS, et al. Morphological study of non-polar (11-20) GaN grown on r-plane (1-102) sapphire. Phys Stat Sol C. 2008;5:1786–1788.

[7] Paduano QS, Weyburne DW, Tomich DH. Growth and properties of m-plane GaN on m-plane sapphire by metal organic chemical vapor deposition. J Cryst Growth. 2013;367:104–109.

[8] Seo YG, Baik Kwang Hyeon, Song H, et al. Orange a-plane InGaN/GaN light-emitting diodes grown on r-plane sapphire substrates. Opt Express. 2011;19:12919–12924.

[9] Park SH, Park J, You DJ, et al. Improved emission efficiency of a-plane GaN light emitting diodes with silica nano-spheres integrated into a-plane GaN buffer layer. Appl Phys Letts. 2012;100:191116-1–191116-4.

[10] Chen CQ, Yang JW, Wang HM, et al. Lateral epitaxial overgrowth of fully coalesced A-Plane GaN on R-Plane sapphire. Jpn J Appl Phys. 2003;42:L640–L642.

[11] Gühne T, Bougrioua Z, Vennéguès P, et al. Cathodoluminescence spectroscopy of epitaxial-lateral-overgrown nonpolar (11-20) and semipolar (11-22) GaN in relation to microstructural characterization. J Appl Phys. 2007;101:113101-1–113101-6.

[12] Oehler F, Sutherland D, Zhu T, et al. Evaluation of growth methods for the heteroepitaxy of non-polar GaN on sapphire by MOVPE. J Cryst Growth. 2014;408:32–41.

[13] Brinkley SE, Lin YD, Chakraborty A, et al. Polarized spontaneous emission from blue-green m-plane GaN-based light emitting diodes. Appl Phys Letts. 2011;98:011110-1–0111103.

[14] Hwang SM, Song H, Seo YG, et al. Enhanced electroluminescence of a-plane InGaN light emitting diodes grown on oxide-patterned r-plane sapphire substrates. Opt Express. 2011;19:23036–23041.

[15] Chiu CH, Kuo SY, Lo MH, et al. Optical properties of a-plane InGaN/GaN multiple quantum wells on r-plane sapphire substrates with different indium compositions. J Appl Phys. 2009;105:063105-1–063105-6.

[16] Zhao Y, Farrell RM, Wu YR, et al. Valence band states and polarized optical emission from nonpolar and semipolar III–nitride quantum well optoelectronic devices. Jap J Appl Phys. 2014;53:100206-1–100206-17.

[17] Oliver RA, Massabuau FCP, Kappers MJ, et al. The impact of gross well width fluctuations on the efficiency of GaN-based light emitting diodes. Appl Phys Letts. 2013;103:141114-1–141114-4.

[18] Vickers ME, Kappers MJ, Smeeton TM, et al. Determination of the indium content and layer thicknesses in InGaN/GaN quantum wells by x-ray scattering. J Appl Phys J Appl Phys. 2003;94:1565–1574.

[19] Vickers ME, Hollander JL, McAleese C, et al. Determination of the composition and thickness of semi-polar and non-polar III-nitride films and quantum wells using X-ray scattering. J Appl Phys. 2012;111:043502-1–043502-13.

[20] Kundys D, Schulz S, Oehler F, et al. Polarized photoluminescence excitation spectroscopy of a-plane InGaN/GaN multiple quantum wells grown on r-plane sapphire . J Appl Phys. 2014;115:113106-1–113106-4.

[21] Nakagawa S, Tsujimura H, Okamoto K, et al. Temperature dependence of polarized electroluminescence from nonpolar m-plane InGaN-based light emitting diodes. Appl Phys Letts. 2007;91:171110-1–17111-3.

[22] Gardner NF, Kim JC, Wierer JJ, et al. Polarization anisotropy in the electroluminescence of m-plane InGaN–GaN multiple-quantum-well light-emitting diodes. Appl Phys Letts. 2005;86:111101-1–111101-3.

[23] Kubota M, Okamoto K, Tanaka T, et al. Temperature dependence of polarized photoluminescence from nonpolar m-plane InGaN multiple quantum wells for blue laser diodes. Appl Phys Letts. 2008;92:011920-1–011920-3.

[24] Graham DM, Soltani-Vala A, Dawson P, et al. Optical and microstructural studies of InGaN/GaN single-quantum-well structures. J Appl Phys. 2005;97:103508-1–103508-5.

[25] Rinke P, Winkelnkemper M, Qteish A, et al. Consistent set of band parameters for the group-III nitrides AlN, GaN, and InN. Phys Rev B. 2008;77:075202-1–075202-15.

[26] Qimin Y, Rinke P, Winkelnkemper M, et al. Band parameters and strain effects in ZnO and group-III nitrides. Semicond Sci Tecnol. 2011;26:014037-1–014037-8.

[27] Marcinkevicius S, Kelchner KM, Kuritzky LY, et al. Photoexcited carrier recombination in wide m-plane InGaN/GaN quantum wells. Appl Phys Letts. 2013;103:111107-1–111107-5.

[28] Watson-Parris D, Godfrey MJ, Dawson P, et al. Carrier localization mechanisms in $In_xGa_{1-x}N$/GaN quantum wells. Phys Rev B. 2011;83:115321-1–115321-7.

[29] Schulz S, Caro MA, Coughlan C, et al. Atomistic analysis of the impact of alloy and well-width fluctuations on the electronic and optical properties of InGaN/GaN quantum wells. Phys Rev B. 2015;91:035439-1–035439-12.

[30] Schulz S, Tanner DP, O'Reilly EP, et al. Structural, electronic, and optical properties of m-plane InGaN/GaN quantum wells: Insights from experiment and atomistic theory. Phys Rev B. 2015;92:235419-1–235419-12.

[31] Davidson JA, Dawson P, Wang T, et al. Photoluminescence studies of InGaN/GaN multi-quantum wells. Semicon Sci Tech. 2001;15:497–506.

[32] Masui H, Yamada H, Iso K, et al. Polarized spontaneous emission from blue-green m -plane GaN-based light emitting diodes. Appl Phys Letts. 2011;98:011110-1–011110-3.

[33] Griffiths James T, Oehler Fabrice, Tang Fengzai, et al. The microstructure of non-polar a-plane InGaN quantum wells. J Appl Phys. 2016;119:175703-1–175703-6.

[34] Tang F, Zhu T, Oehler F, et al. Indium clustering in a-plane InGaN quantum wells as evidenced by atom probe tomography. Appl Phys Letts. 2015;106:072104-1–072104-5.

[35] Riley JR, Detchprohm T, Wetzel C, et al. On the reliable analysis of indium mole fraction within $In_xGa_{1-x}N$ quantum wells using atom probe tomography. Appl Phys Letts. 2014;104:152102–152102.